Acta Cryst E CRYSTALLOGRAPHIC COMMUNICATIONS
ISSN 2056-9890

Synthesis and crystal structures of (2*E*)-1,4-bis(4-chlorophenyl)but-2-ene-1,4-dione and (2*E*)-1,4-bis(4-bromophenyl)but-2-ene-1,4-dione

Dominika N. Lastovickova,[a]‡ John J. La Scala[a] and Rosario C. Sausa[b]*

[a]US Army Research Laboratory, RDRL-WMM-G, Aberdeen Proving Ground, MD 21005, USA, and [b]US Army Research Laboratory, RDRL-WMM-B, Aberdeen Proving Ground, MD 21005, USA. *Correspondence e-mail: rosario.c.sausa.civ@mail.mil

Received 30 January 2018
Accepted 7 February 2018

Edited by M. Zeller, Purdue University, USA

‡ Oak Ridge Institute for Science and Education (ORISE) Postdoctoral Research Fellow.

Keywords: crystal structure; synthesis; 1,4-enedione moiety; bis-halo-enedione; NMR.

CCDC references: 1822698; 1822697

Supporting information: this article has supporting information at journals.iucr.org/e

The molecular structure of (2*E*)-1,4-bis(4-chlorophenyl)but-2-ene-1,4-dione [$C_{16}H_{10}Cl_2O_2$, (**1**)] is composed of two *p*-chlorophenyl rings, each bonded on opposite ends to a near planar 1,4-*trans* enedione moiety [–C(=O)–CH=CH–(C=O)–] [r.m.s. deviation = 0.003 (1) Å]. (2*E*)-1,4-Bis(4-bromophenyl)but-2-ene-1,4-dione [$C_{16}H_{10}Br_2O_2$, (**2**)] has a similar structure to (**1**), but with two *p*-bromophenyl rings and a less planar enedione group [r.m.s. deviation = 0.011 (1) Å]. Both molecules sit on a center of inversion, thus Z' = 0.5. The dihedral angles between the ring and the enedione group are 16.61 (8) and 15.58 (11)° for (**1**) and (**2**), respectively. In the crystal, molecules of (**1**) exhibit C—Cl···Cl type I interactions, whereas molecules of (**2**) present C—Br···Br type II interactions. van der Waals-type interactions contribute to the packing of both molecules, and the packing reveals face-to-face ring stacking with similar interplanar distances of approximately 3.53 Å.

1. Chemical context

The 1,4-enedione moiety [–C(=O)–CH=CH–(C=O)–] occurs in many natural and bioactive compounds, including steroids, antibiotics, and antitumor agents (Koft & Smith, 1982; Ismail *et al.*, 1996; Connolly & Hill, 2010; Fouad *et al.*, 2006; Yang *et al.*, 2013). Its multifunctionality and versatility make it an excellent building block for novel material syntheses. In certain molecules, the facile and reversible *E*/*Z* isomerization of the enedione groups enables them to perform as optical pH and fluorescent sensors (Li *et al.*, 2017). The title compounds (2*E*)-1,4-bis(4-chlorophenyl)but-2-ene-1,4-dione (**1**) and (2*E*)-1,4-bis(4-bromophenyl)but-2-ene-1,4-dione (**2**) exhibit two *p*-halogen phenyl rings, each bonded on opposite ends of the enedione group. We have synthesized these compounds in our laboratory as precursors to 4,4′-(furan-2,5-diyl)dibenzaldehyde cross-linkers. The reduction of the title compounds yields the saturated 1,4-diketones that, under Paal–Knorr reaction conditions, can undergo cyclization to produce the corresponding furans (Sauer *et al.*, 2017). The aryl halides can be subsequently replaced with formyl groups using the Bouveault aldehyde synthesis to generate the targeted 4,4′-(furan-2,5-diyl)dibenzaldehyde cross-linkers, which can be potentially used for non-toxic, isocyanate-free synthesis of polyurethanes.

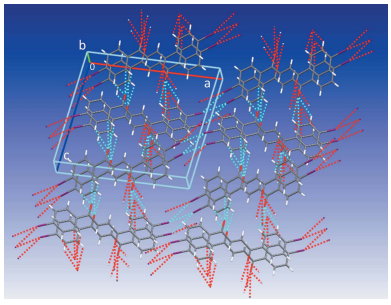

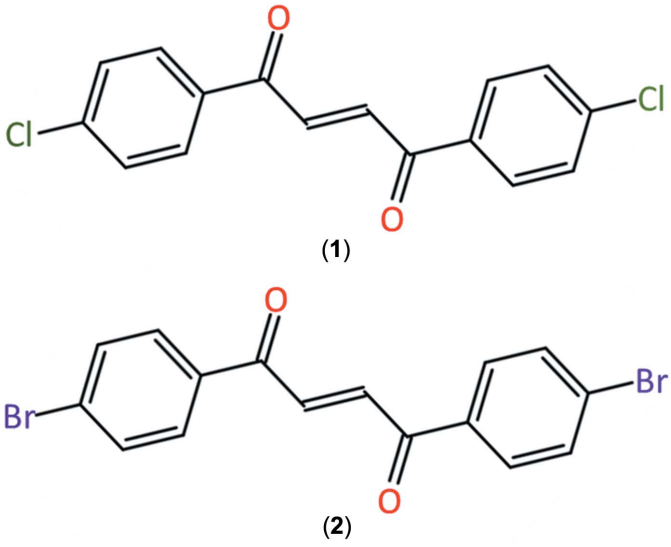

2. Structural commentary

The title compounds exhibit molecular structures typical of biphenyl enedione compounds (Rabinovich *et al.*, 1970; Xu *et al.*, 2013; Li *et al.*, 2014). Bond lengths and angles are in the usual ranges. Fig. 1 shows that the molecules sit on centers of inversion and that the enedione groups adopt a *trans*, near planar configuration [r.m.s deviations = 0.003 (1) and 0.011 (1) Å for (**1**) and (**2**), respectively]. In molecule (**1**), the carbonyl group is twisted slightly out of the chlorophenyl plane, as evidenced by the torsion angles C6—C1—C7—O1 [−15.6 (3)°] and C2—C1—C7—O1 [163.9 (2)°]. Molecule (**2**) shows a similar conformation with torsion angles of 14.5 (4) and −164.7 (3)° for the corresponding atoms of the inverted

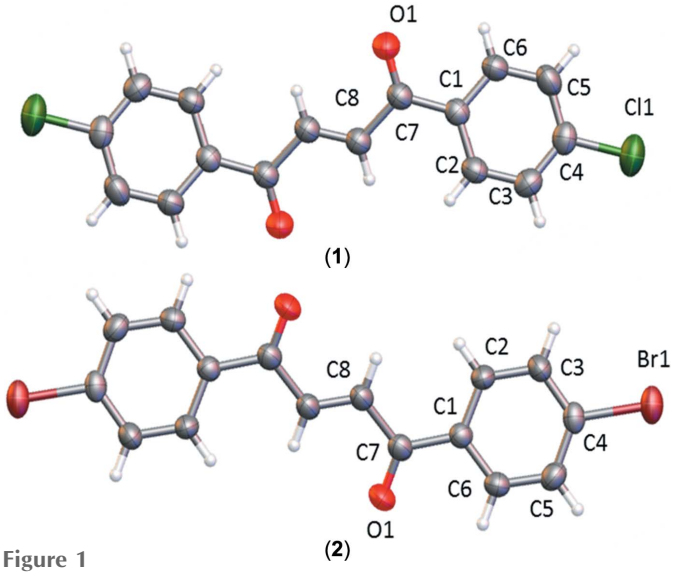

Figure 1
Molecular conformation and atom-numbering scheme of (**1**) (top) and (**2**) (bottom). The non-labeled atoms are generated by symmetry operation (−*x*, 1 − *y*, 1 − *z*) for (**1**) and (1 − *x*, −*y*,1 − *z*) for (**2**). Non-hydrogen atoms are shown as 50% probability displacement ellipsoids.

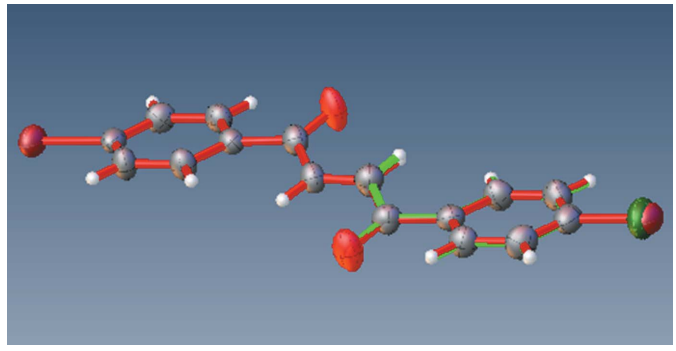

Figure 2
Superimposition of structure (**1**) (green) onto the inverted structure of (**2**) (red). Only the asymmetric unit of (**1**) is presented for clarity.

asymmetric unit (−*x* + 1, −*y*, −*z* + 1). The chlorophenyl ring planes form a dihedral angle of 16.61 (8)° with respect to the enedione plane (O1–C7–C8–C8′–C7′–O1′) in (**1**), whereas the bromophenyl ring planes form a dihedral angle of 15.58 (11)° relative to the enedione plane in (**2**). Both molecules exhibit a pair of short intramolecular H···H contacts [(**1**): H2···H8 = H2^{i}···H8^{i} = 2.127 (2) Å; symmetry code (i): −*x*, 1 − *y*, 1 − *z*; and (**2**): H2···H8 = H2^{ii}···H8^{ii} = 2.113 (3) Å; symmetry code: (ii) 1 − *x*, −y, 1 − *z*], possibly resulting from steric compression of the large phenyl halogen groups. A best fit of all symmetry independent atoms of both molecules (see Fig. 2) yields an r.m.s. deviation of 0.05 Å.

3. Supramolecular features

Contacts between the O atoms and H atoms of adjacent molecules [O1···H3^{i} = 3.329 (2) Å; symmetry code: (i) −1 + *x*, 1 + *y*, *z*] and between the Cl atoms and Cl atoms of adjacent molecules [Cl1···Cl1^{ii} = 3.3841 (1) Å; symmetry code: (ii) 2 − *x*, −*y*, −*z*] contribute to the intermolecular interactions of (**1**) (see Fig. 3). The short Cl···Cl distances are approximately 0.3 Å shorter than double the Cl van der Waals radius of 3.64 Å (Alvarez, 2013). The molecules feature type I, C_w—Cl_x···Cl_y—C_z interactions, where θ_1 = angle C_w—Cl_x···Cl_y, θ_2 = angle Cl_x···Cl_y—C_z, and $|\theta_1 - \theta_2| = 0$ ($\theta_1 = \theta_2$, approximately 157°) (see Fig. 4), suggesting that the Cl atoms minimize repulsion by interfacing the neutral regions of their electrostatic potential surfaces (Desiraju & Parthasarathy, 1989; Mukherjee & Desiraju, 2014). Unlike (**1**), (**2**) exhibits trifurcated contacts between the O atoms and H and C atoms of adjacent molecules [O1···H2^{iii} = 2.616 (2) Å, O1···H3^{iii} = 2.711 (2) Å, and O1···C2^{iii} = 3.194 (3) Å; symmetry code: (iii) *x*, $\frac{1}{2}$ − *y*, $\frac{1}{2}$ + *z*]. Furthermore, the Br atoms form bifurcated contacts with the Br atoms of adjacent molecules [Br1···Br1^{v} = Br1···Br1^{v} = 3.662 (1) Å; symmetry codes: (iv) −*x*, $-\frac{1}{2}$ + *y*, $\frac{3}{2}$ − *z*; (v) −*x*, $\frac{1}{2}$ + *y*, $\frac{3}{2}$ − *z*] (see Fig. 5). Inspection of the C—Br···Br—C angles, reveals that the molecules exhibit type II interactions ($|\theta_1 - \theta_2| \geq 30°$, where θ_1 (164.58°) − θ_2 (121.71°) = 42.87°, suggesting the electrophilic region of one Br atom approaches the nucleophilic region of the companion Br atom, unlike the Cl···Cl interactions (Mukherjee & Desiraju, 2014;

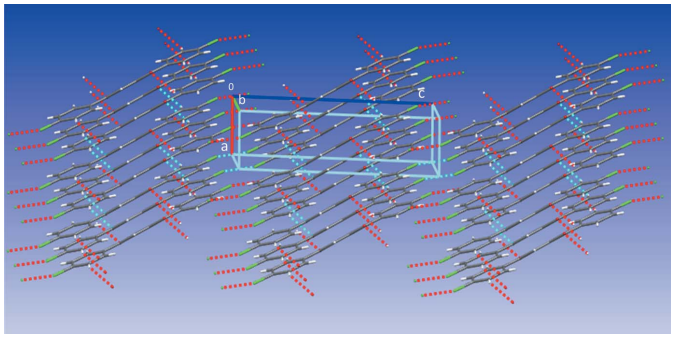

Figure 3
Crystal packing of (**1**) along the vicinity of the *a* axis. Dashed lines depict Cl1···Cl1^{i} and O1···H3^{ii} interactions [symmetry codes: (i) $2-x, -y, -z$; (ii) $-1+x, 1+y, z$].

Tothadi *et al.*, 2013; Nuzzo *et al.*, 2017). The chlorophenyl rings (**1**) are stacked in close proximity along the vicinity of the *a* axis with an interplanar separation of 3.528 Å [centroid-to-centroid distance = 3.946 (1) Å] (see Figs. 4 and 5). Similarly, the bromo phenyl rings of (**2**) stack along the vicinity of the *a* axis with an interplanar separation of 3.525 Å [centroid-to-centroid distance = 3.994 (1) Å], but in a crisscross-like pattern when viewed along the *c* axis (see Figs. 3 and 5). The intersecting ring planes subtend dihedral angles of 48.09 (6)°.

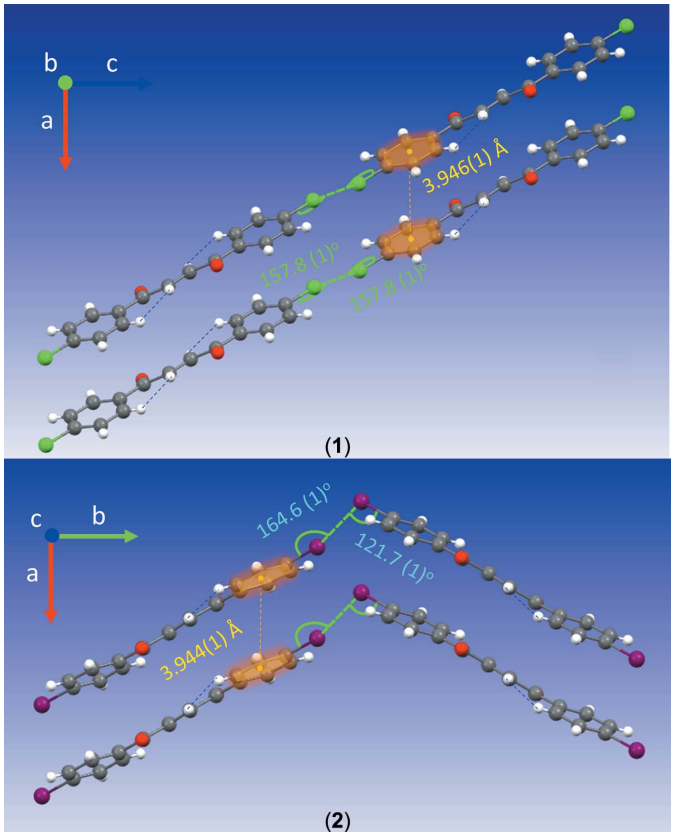

Figure 4
Molecular conformations of (**1**) and (**2**) viewed along the *b* and *c* axes, respectively, showing type I and II halogen interactions, centroid-to-centroid distances, and short intramolecular H···H interactions.

4. Database survey

A search of the Cambridge Structural Database (CSD web interface; Groom *et al.*, 2016) and the Crystallography Open Database (Gražulis *et al.*, 2009) yields the crystal structures of a number of compounds containing the 1,4-enedione moiety. For examples, see Rabinovich *et al.* (1970), Xu *et al.* (2013), Li *et al.* (2014), Deng *et al.* (2012); Gao *et al.* (2010), and Wu *et al.* (2011). The compounds *trans*-1,2-diphenylethylene (**3**) (Xu *et al.*, 2013; CCDC 918566, BZOYEY01) and *cis*-1,2-dichlorobenzoylethylene (**4**) (Rabinovich *et al.*, 1970; CCDC 112151, CBOZET) merit discussion because the former has a similar structure to the title compounds, whereas the latter is a stereoisomer of (**1**). The title compounds adopt an *E* configuration, similar to (**3**). They contain halogen atoms in the *para* position of the phenyl groups, unlike (**3**), but the rings are nearly planar as are those of (**3**), whose r.m.s value = 0.008 Å. The r.m.s. value, reflecting the planarity of the enedione moiety, in (**1**) is different to that of (**3**) (0.003 *vs* 0.0035 Å), and the value determined for (**2**) (0.011 Å). The dihedral angles between the ring planes of (**1**) and (**2**) are nearly identical to those of (**3**) [16° (average) *vs* 15.7 (1)°]. Unlike (**1**), its diastereomer (**4**) does not exhibit a planar enedione moiety and its near planar chlorophenyl rings (r.m.s deviation = 0.018 Å) form a dihedral angle of 77.4 (3)° with respect to each other. Superimposition of atom C1 of the *E*/*Z* diastereomers through the C7, Cl1, and O1 atoms yields an r.m.s. deviation of 0.033 Å. The remaining parts of the molecules are twisted from each other, with the planes containing the chlorophenyl group and adjoining carbonyl group of each stereoisomer forming a dihedral angle of approximately 79°.

5. Synthesis and crystallization

The title compounds were synthesized following a modified literature procedure (Sauer *et al.*, 2017). The reactions were

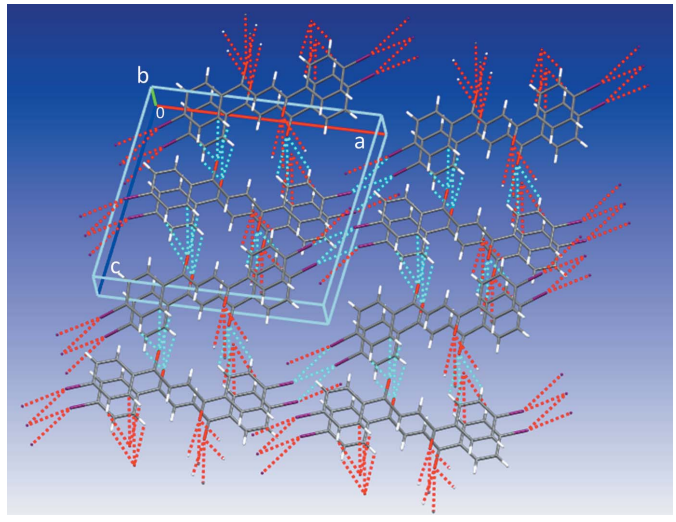

Figure 5
Crystal packing of (**2**) along the *b* axis. Dashed blue lines represent bifurcated Br1···Br1^{iv,v} interactions [symmetry codes: (iv) $-x, -\frac{1}{2}+y, \frac{3}{2}-z$; (v) $-x, \frac{1}{2}+y, \frac{3}{2}-z$] and trifurcated interactions involving the O1 atoms.

Table 1
Experimental details.

	(**1**)	(**2**)
Crystal data		
Chemical formula	$C_{16}H_{10}Cl_2O_2$	$C_{16}H_{10}Br_2O_2$
M_r	305.14	394.06
Crystal system, space group	Triclinic, $P\overline{1}$	Monoclinic, $P2_1/c$
Temperature (K)	298	298
a, b, c (Å)	3.9455 (3), 6.0809 (5), 14.6836 (11)	14.4391 (7), 3.9937 (2), 12.7244 (7)
α, β, γ (°)	82.653 (6), 88.638 (6), 84.601 (7)	90, 97.827 (5), 90
V (Å^3)	347.82 (5)	726.92 (7)
Z	1	2
Radiation type	Mo $K\alpha$	Mo $K\alpha$
μ (mm^{-1})	0.46	5.57
Crystal size (mm)	0.34 × 0.22 × 0.15	0.35 × 0.14 × 0.12
Data collection		
Diffractometer	Agilent SuperNova, Dualflex, EosS2	Agilent SuperNova, Dualflex, EosS2
Absorption correction	Multi-scan (*CrysAlis PRO*; Bourhis *et al.*, 2015)	Multi-scan (*CrysAlis PRO*; Bourhis *et al.*, 2015)
T_{min}, T_{max}	0.928, 1.000	0.370, 1.000
No. of measured, independent and observed [$I > 2\sigma(I)$] reflections	5641, 1416, 1256	6231, 1470, 1228
R_{int}	0.023	0.031
(sin $\theta/\lambda)_{max}$ (Å^{-1})	0.625	0.625
Refinement		
$R[F^2 > 2\sigma(F^2)]$, $wR(F^2)$, S	0.048, 0.104, 1.16	0.029, 0.065, 1.08
No. of reflections	1416	1470
No. of parameters	91	92
H-atom treatment	H-atom parameters constrained	H-atom parameters constrained
$\Delta\rho_{max}$, $\Delta\rho_{min}$ (e Å^{-3})	0.18, −0.20	0.36, −0.43

Computer programs: *CrysAlis PRO* (Rigaku OD, 2015), *SHELXT* (Sheldrick, 2015*a*), *SHELXL* (Sheldrick, 2015*b*), *OLEX2* (Dolomanov *et al.*, 2009) and *Mercury* (Macrae *et al.*, 2008).

run 'neat' with chloro- or bromobenzene used in excess and serving also as the reaction solvent. Under a stream of nitrogen, aluminum chloride (3.6 g, 27 mmol, 2.9 equiv.) was dissolved in chloro- or bromobenzene (9.0 and 9.3 ml, respectively, 89 mmol, 9.6 equiv.) at room temperature. The reaction mixture was subsequently cooled to 273 K and fumaryl chloride (1.0 ml, 9.3 mmol, 1.0 equiv.) was added dropwise under constant stirring, at which point an instantaneous color change from clear to deep red was observed. The reaction mixture was then heated to 333 K for 2–4 days until fumaryl chloride was no longer detected on a TLC plate (SiO_2, DCM). At the conclusion of the reaction, the mixture was cooled to room temperature, poured into ice-cold aqueous 1 *M* HCl, and extracted several times with DCM. The combined organic layers were washed with 0.5 *M* NaOH and dried over Na_2SO_4, and the volatiles were removed under reduced pressure. The resulting red–brown solid was recrystallized in DCM, further purified with a series of cold DCM washes, and dried under reduced pressure, affording either compound (**1**) (burnt orange solid, 1.5 g, 4.9 mmol, 53% yield) or (**2**) (yellow solid, 1.9 g, 4.8 mmol, 50% yield). Slow evaporation of DCM solutions saturated with either (**1**) or (**2**) yielded single crystals suitable for X-ray diffraction.

NMR spectra were recorded on a Bruker 400 MHz spectrometer. Chemical shifts (δ) are given in ppm and are referenced to tetramethylsilane (TMS) using the residual solvent (^{1}H: $CDCl_3$, 7.26 ppm; ^{13}C: $CDCl_3$, 77.16 ppm). (**1**): ^{1}H NMR ($CDCl_3$, 400.13 MHz): δ 7.51 (*d*, *J* = 8.6 Hz, 4H), 7.97 (*s*, 2H), 8.00 (*d*, *J* = 8.6 Hz, 4H) ppm. ^{13}C NMR ($CDCl_3$, 100.62 MHz): δ 129.48, 130.40, 135.06, 135.31, 140.77, 188.51 ppm. (**2**): ^{1}H NMR ($CDCl_3$, 400.13 MHz): δ 7.67 (*d*, *J* = 8.6 Hz, 4H), 7.92 (*d*, *J* = 8.6 Hz, 4H), 7.96 (s, 2H) ppm. ^{13}C NMR ($CDCl_3$, 100.62 MHz): δ 129.53, 130.44, 132.45, 135.03, 135.69, 188.69 ppm.

6. Refinement

Crystal data, data collection and structure refinement details are summarized in Table 1. The hydrogen atoms of both compounds were refined using a riding model with C—H = 0.93 Å and U_{iso}(H) = 1.2U_{eq}(C).

Funding information

This research was supported in part by an appointment to the Postgraduate Research Participation Program at the US Army Research Laboratory (USARL) by the Oak Ridge Institute for Science and Education through an interagency agreement between the US Department of Energy and the USARL.

References

Alvarez, S. (2013). *Dalton Trans.* **42**, 8617–8636.
Bourhis, L. J., Dolomanov, O. V., Gildea, R. J., Howard, J. A. K. & Puschmann, H. (2015). *Acta Cryst.* A**71**, 59–75.
Connolly, J. D. & Hill, R. A. (2010). *Nat. Prod. Rep.* **27**, 79–132.
Deng, C., Yang, Y., Gao, M., Zhu, Y.-P., Wu, A.-X., Ma, J.-R. & Yin, G.-D. (2012). *Tetrahedron*, **68**, 3828–3834.

Desiraju, G. R. & Parthasarathy, R. (1989). *J. Am. Chem. Soc.* **111**, 8725–8726.
Dolomanov, O. V., Bourhis, L. J., Gildea, R. J., Howard, J. A. K. & Puschmann, H. (2009). *J. Appl. Cryst.* **42**, 339–341.
Fouad, M., Edrada, R. A., Ebel, R., Wray, V., Müller, W. E. G., Lin, W. H. & Proksch, P. J. (2006). *J. Nat. Prod.* **69**, 211–218.
Gao, M., Yang, Y., Wu, Y.-D., Deng, C., Cao, L.-P., Meng, X. G. & Wu, A.-X. (2010). *J. Org. Chem.* **12**(8), 1856–1859.
Gražulis, S., Chateigner, D., Downs, R. T., Yokochi, A. F. T., Quirós, M., Lutterotti, L., Manakova, E., Butkus, J., Moeck, P. & Le Bail, A. (2009). *J. Appl. Cryst.* **42**, 726–729.
Groom, C. R., Bruno, I. J., Lightfoot, M. P. & Ward, S. C. (2016). *Acta Cryst.* B**72**, 171–179.
Ismail, K. A., El-Tombary, A. A., Aboulwafa, O. M., Omar, A. M. E. & El-Rewini, S. H. (1996). *Arch. Pharm. Pharm. Med. Chem.* **329**, 433–437.
Koft, E. R. & Smith, A. B. (1982). *J. Am. Chem. Soc.* **104**, 2659–2661.
Li, S.-Y., Wang, X.-B., Jiang, N. & Kong, L.-Y. (2014). *Eur. J. Org. Chem.* pp. 8035–8039.
Li, M., Wang, Y. X., Wang, J. & Chen, Y. (2017). *J. Mater. Chem.* **C5**, 3408–3414.
Macrae, C. F., Bruno, I. J., Chisholm, J. A., Edgington, P. R., McCabe, P., Pidcock, E., Rodriguez-Monge, L., Taylor, R., van de Streek, J. & Wood, P. A. (2008). *J. Appl. Cryst.* **41**, 466–470.
Mukherjee, A. & Desiraju, G. R. (2014). *IUCrJ*, **1**, 49–60.
Nuzzo, S., Twamley, B. & Baker, R. J. (2017). *J. Chem. Crystallogr.* **47**, 182–186.
Rabinovich, D., Schmidt, G. M. J. & Shaked, D. (1970). *J. Chem. Soc. B*, pp. 17–24.
Rigaku OD (2015). *CrysAlis PRO*. Rigaku Oxford Diffraction Ltd, Yarnton, England.
Sauer, B., Skinner-Adams, T. S., Bouchut, A., Chua, M. J., Pierrot, C., Erdmann, F., Robaa, D., Schmidt, M., Khalife, J., Andrews, K. T. & Sippl, W. (2017). *Eur. J. Med. Chem.* **127**, 22–40.
Sheldrick, G. M. (2015*a*). *Acta Cryst.* A**71**, 3–8.
Sheldrick, G. M. (2015*b*). *Acta Cryst.* C**71**, 3–8.
Tothadi, S., Joseph, S. & Desiraju, G. R. (2013). *Cryst. Growth Des.* **13**, 3242–3254.
Wu, L., Deng, C. & Yang, Y. (2011). *Acta Cryst.* E**67**, o1499.
Xu, K., Fang, Y., Yan, Z., Zha, Z. & Wang, Z. (2013). *Org. Lett.* **15**, 2148–2151.
Yang, Y., Ni, F., Shu, W.-M., Yu, S.-B., Gao, M. & Wu, A.-X. (2013). *J. Org. Chem.* **78**, 5418–5426.

supporting information

Acta Cryst. (2018). E**74**, 352-356 [https://doi.org/10.1107/S205698901800230X]

Synthesis and crystal structures of (2*E*)-1,4-bis(4-chlorophenyl)but-2-ene-1,4-dione and (2*E*)-1,4-bis(4-bromophenyl)but-2-ene-1,4-dione

Dominika N. Lastovickova, John J. La Scala and Rosario C. Sausa

Computing details

For both structures, data collection: *CrysAlis PRO* (Rigaku OD, 2015); cell refinement: *CrysAlis PRO* (Rigaku OD, 2015); data reduction: *CrysAlis PRO* (Rigaku OD, 2015); program(s) used to solve structure: SHELXT (Sheldrick, 2015a); program(s) used to refine structure: *SHELXL* (Sheldrick, 2015b); molecular graphics: *OLEX2* (Dolomanov *et al.*, 2009). Software used to prepare material for publication: *Mercury* (Macrae *et al.*, 2008) for (1); *OLEX2* (Dolomanov *et al.*, 2009) for (2).

(2*E*)-1,4-Bis(4-chlorophenyl)but-2-ene-1,4-dione (1)

Crystal data

$C_{16}H_{10}Cl_2O_2$
M_r = 305.14
Triclinic, $P\overline{1}$
a = 3.9455 (3) Å
b = 6.0809 (5) Å
c = 14.6836 (11) Å
α = 82.653 (6)°
β = 88.638 (6)°
γ = 84.601 (7)°
V = 347.82 (5) Å^3
Z = 1
$F(000)$ = 156
D_x = 1.457 Mg m^{-3}
Mo $K\alpha$ radiation, λ = 0.71073 Å
Cell parameters from 2009 reflections
θ = 2.8–26.3°
μ = 0.46 mm^{-1}
T = 298 K
Irregular, orange
0.34 × 0.22 × 0.15 mm

Data collection

Agilent SuperNova, Dualflex, EosS2 diffractometer
Detector resolution: 8.0945 pixels mm^{-1}
ω scans
Absorption correction: multi-scan (CrysAlisPro; Bourhis *et al.*, 2015)
T_{min} = 0.928, T_{max} = 1.000
5641 measured reflections
1416 independent reflections
1256 reflections with $I > 2\sigma(I)$
R_{int} = 0.023
θ_{max} = 26.4°, θ_{min} = 2.8°
h = −4→4
k = −7→7
l = −18→18

Refinement

Refinement on F^2
Least-squares matrix: full
$R[F^2 > 2\sigma(F^2)]$ = 0.048
$wR(F^2)$ = 0.104
S = 1.16
1416 reflections
91 parameters
0 restraints
Hydrogen site location: inferred from neighbouring sites
H-atom parameters constrained
$w = 1/[\sigma^2(F_o^2) + (0.0335P)^2 + 0.118P]$ where $P = (F_o^2 + 2F_c^2)/3$
$(\Delta/\sigma)_{max} < 0.001$
$\Delta\rho_{max}$ = 0.18 e Å^{-3}
$\Delta\rho_{min}$ = −0.19 e Å^{-3}

Special details

Geometry. All esds (except the esd in the dihedral angle between two l.s. planes) are estimated using the full covariance matrix. The cell esds are taken into account individually in the estimation of esds in distances, angles and torsion angles; correlations between esds in cell parameters are only used when they are defined by crystal symmetry. An approximate (isotropic) treatment of cell esds is used for estimating esds involving l.s. planes.

Fractional atomic coordinates and isotropic or equivalent isotropic displacement parameters (Å²)

	x	*y*	*z*	U_{iso}*/U_{eq}
C1	0.3800 (5)	0.4949 (3)	0.30832 (13)	0.0411 (4)
C2	0.5146 (5)	0.2732 (3)	0.31865 (14)	0.0482 (5)
H2	0.493021	0.185559	0.374837	0.058*
C3	0.6788 (6)	0.1826 (4)	0.24675 (15)	0.0529 (5)
H3	0.771626	0.035173	0.254438	0.063*
C4	0.7048 (5)	0.3111 (4)	0.16369 (14)	0.0500 (5)
C5	0.5749 (6)	0.5314 (4)	0.15096 (15)	0.0559 (6)
H5	0.595485	0.617285	0.094315	0.067*
C6	0.4149 (5)	0.6214 (3)	0.22341 (14)	0.0495 (5)
H6	0.327970	0.770037	0.215556	0.059*
C7	0.2047 (5)	0.6004 (3)	0.38415 (14)	0.0459 (5)
C8	0.0820 (5)	0.4582 (3)	0.46605 (13)	0.0452 (5)
H8	0.123290	0.304322	0.469025	0.054*
Cl1	0.90353 (18)	0.19244 (12)	0.07252 (4)	0.0768 (3)
O1	0.1558 (5)	0.8021 (2)	0.38003 (11)	0.0699 (5)

Atomic displacement parameters (Å²)

	U^{11}	U^{22}	U^{33}	U^{12}	U^{13}	U^{23}
C1	0.0389 (10)	0.0429 (10)	0.0419 (10)	−0.0081 (8)	−0.0005 (8)	−0.0038 (8)
C2	0.0565 (13)	0.0421 (11)	0.0450 (11)	−0.0066 (9)	0.0017 (9)	−0.0003 (9)
C3	0.0558 (13)	0.0447 (11)	0.0587 (13)	−0.0013 (10)	−0.0009 (10)	−0.0115 (10)
C4	0.0463 (12)	0.0595 (13)	0.0471 (12)	−0.0076 (10)	0.0021 (9)	−0.0164 (10)
C5	0.0616 (14)	0.0622 (13)	0.0413 (11)	−0.0054 (11)	0.0049 (10)	0.0017 (10)
C6	0.0539 (12)	0.0437 (11)	0.0481 (12)	−0.0008 (9)	0.0031 (9)	0.0017 (9)
C7	0.0480 (11)	0.0440 (11)	0.0450 (11)	−0.0066 (9)	0.0022 (9)	−0.0017 (8)
C8	0.0477 (12)	0.0431 (10)	0.0440 (11)	−0.0046 (9)	0.0015 (8)	−0.0023 (8)
Cl1	0.0799 (5)	0.0926 (5)	0.0621 (4)	−0.0021 (4)	0.0148 (3)	−0.0326 (3)
O1	0.1034 (14)	0.0410 (8)	0.0617 (10)	−0.0006 (8)	0.0245 (9)	−0.0015 (7)

Geometric parameters (Å, º)

C1—C2	1.392 (3)	C4—Cl1	1.737 (2)
C1—C6	1.390 (3)	C5—H5	0.9300
C1—C7	1.481 (3)	C5—C6	1.372 (3)
C2—H2	0.9300	C6—H6	0.9300
C2—C3	1.374 (3)	C7—C8	1.488 (3)
C3—H3	0.9300	C7—O1	1.218 (2)
C3—C4	1.369 (3)	C8—C8^{i}	1.307 (4)

C4—C5	1.379 (3)	C8—H8	0.9300
C2—C1—C7	122.61 (18)	C4—C5—H5	120.6
C6—C1—C2	118.30 (19)	C6—C5—C4	118.8 (2)
C6—C1—C7	119.08 (18)	C6—C5—H5	120.6
C1—C2—H2	119.6	C1—C6—H6	119.3
C3—C2—C1	120.72 (19)	C5—C6—C1	121.3 (2)
C3—C2—H2	119.6	C5—C6—H6	119.3
C2—C3—H3	120.3	C1—C7—C8	119.63 (17)
C4—C3—C2	119.4 (2)	O1—C7—C1	120.95 (18)
C4—C3—H3	120.3	O1—C7—C8	119.41 (19)
C3—C4—C5	121.4 (2)	C7—C8—H8	118.8
C3—C4—Cl1	118.98 (17)	C8^{i}—C8—C7	122.3 (2)
C5—C4—Cl1	119.60 (17)	C8^{i}—C8—H8	118.8
C1—C2—C3—C4	−1.1 (3)	C4—C5—C6—C1	−0.4 (3)
C1—C7—C8—C8^{i}	−178.2 (2)	C6—C1—C2—C3	0.3 (3)
C2—C1—C6—C5	0.5 (3)	C6—C1—C7—C8	163.48 (18)
C2—C1—C7—C8	−17.0 (3)	C6—C1—C7—O1	−15.6 (3)
C2—C1—C7—O1	163.9 (2)	C7—C1—C2—C3	−179.24 (19)
C2—C3—C4—C5	1.2 (3)	C7—C1—C6—C5	−179.94 (19)
C2—C3—C4—Cl1	−178.37 (16)	Cl1—C4—C5—C6	179.15 (16)
C3—C4—C5—C6	−0.4 (3)	O1—C7—C8—C8^{i}	0.9 (4)

Symmetry code: (i) −*x*, −*y*+1, −*z*+1.

(2*E*)-1,4-Bis(4-bromophenyl)but-2-ene-1,4-dione (2)

Crystal data

$C_{16}H_{10}Br_2O_2$
M_r = 394.06
Monoclinic, $P2_1/c$
a = 14.4391 (7) Å
b = 3.9937 (2) Å
c = 12.7244 (7) Å
β = 97.827 (5)°
V = 726.92 (7) Å^3
Z = 2
$F(000)$ = 384
D_x = 1.800 Mg m^{-3}
Mo $K\alpha$ radiation, λ = 0.71073 Å
Cell parameters from 2527 reflections
θ = 2.9–26.2°
μ = 5.57 mm^{-1}
T = 298 K
Irregular, yellow
0.35 × 0.14 × 0.12 mm

Data collection

Agilent SuperNova, Dualflex, EosS2 diffractometer
Detector resolution: 8.0945 pixels mm^{-1}
ω scans
Absorption correction: multi-scan (CrysAlisPro; Bourhis *et al.*, 2015)
T_{min} = 0.370, T_{max} = 1.000
6231 measured reflections
1470 independent reflections
1228 reflections with $I > 2\sigma(I)$
R_{int} = 0.031
θ_{max} = 26.4°, θ_{min} = 2.9°
h = −18→18
k = −4→4
l = −15→15

Refinement

Refinement on F^2
Least-squares matrix: full
$R[F^2 > 2\sigma(F^2)] = 0.029$
$wR(F^2) = 0.065$
$S = 1.08$
1470 reflections
92 parameters
0 restraints
Hydrogen site location: inferred from neighbouring sites
H-atom parameters constrained
$w = 1/[\sigma^2(F_o^2) + (0.0234P)^2 + 0.4382P]$ where $P = (F_o^2 + 2F_c^2)/3$
$(\Delta/\sigma)_{max} < 0.001$
$\Delta\rho_{max} = 0.36$ e Å^{-3}
$\Delta\rho_{min} = -0.43$ e Å^{-3}
Extinction correction: SHELXL-2016/4 (Sheldrick, 2015b), $Fc^*=kFc[1+0.001xFc^2\lambda^3/\sin(2\theta)]^{-1/4}$
Extinction coefficient: 0.0047 (8)

Special details

Geometry. All esds (except the esd in the dihedral angle between two l.s. planes) are estimated using the full covariance matrix. The cell esds are taken into account individually in the estimation of esds in distances, angles and torsion angles; correlations between esds in cell parameters are only used when they are defined by crystal symmetry. An approximate (isotropic) treatment of cell esds is used for estimating esds involving l.s. planes.

Fractional atomic coordinates and isotropic or equivalent isotropic displacement parameters (Å²)

	x	*y*	*z*	U_{iso}*/U_{eq}
Br1	0.06905 (2)	0.86344 (8)	0.66837 (3)	0.05337 (16)
C1	0.31059 (19)	0.3876 (7)	0.5110 (2)	0.0355 (6)
C2	0.3212 (2)	0.4543 (8)	0.6188 (2)	0.0444 (7)
H2	0.377230	0.400535	0.660470	0.053*
C3	0.2503 (2)	0.5990 (8)	0.6653 (2)	0.0471 (8)
H3	0.258517	0.646056	0.737543	0.057*
C4	0.1673 (2)	0.6726 (6)	0.6034 (2)	0.0391 (7)
C5	0.1538 (2)	0.6073 (7)	0.4962 (2)	0.0463 (7)
H5	0.097052	0.657253	0.455312	0.056*
C6	0.2258 (2)	0.4666 (8)	0.4507 (2)	0.0422 (7)
H6	0.217497	0.423632	0.378154	0.051*
C7	0.3859 (2)	0.2399 (8)	0.4570 (2)	0.0418 (7)
C8	0.4672 (2)	0.0760 (7)	0.5218 (2)	0.0410 (7)
H8	0.471561	0.081856	0.595399	0.049*
O1	0.38162 (17)	0.2478 (7)	0.36132 (17)	0.0665 (7)

Atomic displacement parameters (Å²)

	U^{11}	U^{22}	U^{33}	U^{12}	U^{13}	U^{23}
Br1	0.0433 (2)	0.0504 (2)	0.0706 (3)	0.00725 (15)	0.02309 (16)	0.00106 (17)
C1	0.0354 (15)	0.0380 (14)	0.0334 (15)	−0.0010 (12)	0.0057 (12)	0.0011 (12)
C2	0.0380 (17)	0.0601 (19)	0.0340 (16)	0.0088 (14)	0.0012 (13)	−0.0001 (14)
C3	0.0465 (18)	0.0598 (19)	0.0359 (16)	0.0119 (15)	0.0082 (13)	−0.0026 (15)
C4	0.0371 (16)	0.0344 (15)	0.0487 (18)	0.0009 (12)	0.0158 (13)	0.0028 (13)
C5	0.0371 (16)	0.0514 (18)	0.0487 (18)	0.0054 (14)	0.0002 (13)	0.0034 (15)
C6	0.0439 (17)	0.0491 (17)	0.0328 (15)	0.0031 (14)	0.0030 (13)	−0.0006 (13)
C7	0.0395 (16)	0.0480 (16)	0.0382 (17)	−0.0016 (13)	0.0060 (13)	−0.0057 (13)
C8	0.0364 (16)	0.0514 (18)	0.0357 (15)	−0.0005 (13)	0.0060 (12)	−0.0064 (14)
O1	0.0591 (15)	0.109 (2)	0.0322 (12)	0.0232 (14)	0.0078 (11)	−0.0071 (12)

Geometric parameters (Å, º)

Br1—C4	1.896 (3)	C4—C5	1.376 (4)
C1—C2	1.385 (4)	C5—H5	0.9300
C1—C6	1.390 (4)	C5—C6	1.377 (4)
C1—C7	1.485 (4)	C6—H6	0.9300
C2—H2	0.9300	C7—C8	1.492 (4)
C2—C3	1.378 (4)	C7—O1	1.211 (3)
C3—H3	0.9300	C8—C8^{i}	1.310 (5)
C3—C4	1.374 (4)	C8—H8	0.9300
C2—C1—C6	118.3 (3)	C4—C5—H5	120.6
C2—C1—C7	123.1 (3)	C4—C5—C6	118.8 (3)
C6—C1—C7	118.7 (3)	C6—C5—H5	120.6
C1—C2—H2	119.4	C1—C6—H6	119.4
C3—C2—C1	121.2 (3)	C5—C6—C1	121.3 (3)
C3—C2—H2	119.4	C5—C6—H6	119.4
C2—C3—H3	120.5	C1—C7—C8	119.3 (2)
C4—C3—C2	119.0 (3)	O1—C7—C1	121.0 (3)
C4—C3—H3	120.5	O1—C7—C8	119.7 (3)
C3—C4—Br1	118.8 (2)	C7—C8—H8	119.0
C3—C4—C5	121.5 (3)	C8^{i}—C8—C7	121.9 (4)
C5—C4—Br1	119.7 (2)	C8^{i}—C8—H8	119.0
Br1—C4—C5—C6	−179.6 (2)	C3—C4—C5—C6	−0.4 (5)
C1—C2—C3—C4	1.0 (5)	C4—C5—C6—C1	0.6 (5)
C1—C7—C8—C8^{i}	175.8 (3)	C6—C1—C2—C3	−0.8 (5)
C2—C1—C6—C5	−0.1 (4)	C6—C1—C7—C8	−164.8 (3)
C2—C1—C7—C8	16.0 (4)	C6—C1—C7—O1	14.5 (4)
C2—C1—C7—O1	−164.7 (3)	C7—C1—C2—C3	178.4 (3)
C2—C3—C4—Br1	178.8 (2)	C7—C1—C6—C5	−179.3 (3)
C2—C3—C4—C5	−0.5 (5)	O1—C7—C8—C8^{i}	−3.5 (6)

Symmetry code: (i) −*x*+1, −*y*, −*z*+1.